SINTEF
PROCEEDINGS
2

Proceedings of the 12th International Conference on Computational Fluid Dynamics in the Oil & Gas, Metallurgical and Process Industries

Progress in Applied CFD – CFD2017

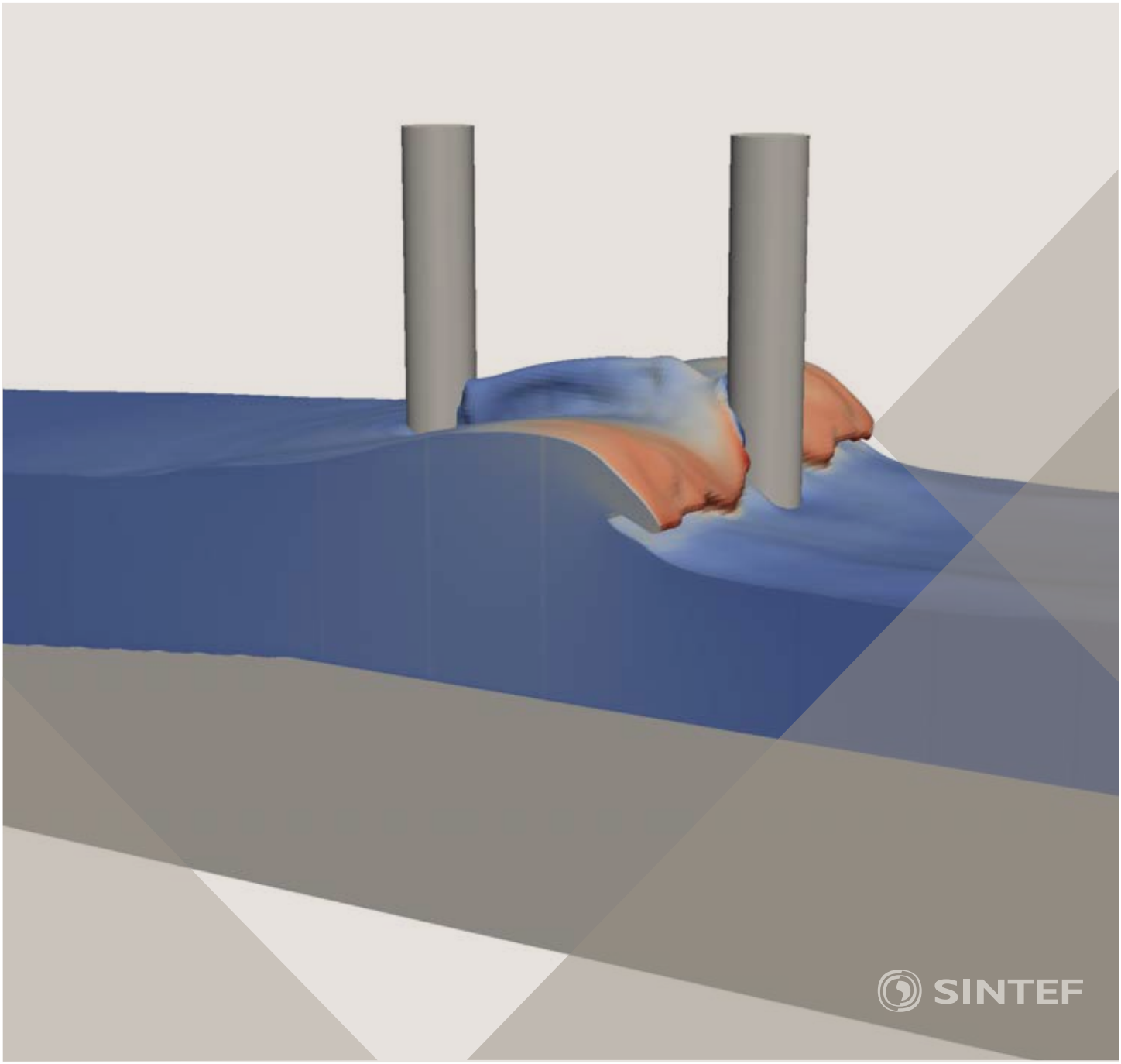

SINTEF Proceedings

Editors:
Jan Erik Olsen and Stein Tore Johansen

Progress in Applied CFD – CFD2017

Proceedings of the 12th International Conference on Computational Fluid Dynamics in the Oil & Gas, Metallurgical and Process Industries

SINTEF Academic Press

SINTEF Proceedings no 2
Editors: Jan Erik Olsen and Stein Tore Johansen
Progress in Applied CFD – CFD2017
Selected papers from 10th International Conference on Computational Fluid Dynamics in the Oil & Gas, Metallurgical and Process Industries

Key words:
CFD, Flow, Modelling

Cover, illustration: Arun Kamath

ISSN 2387-4295 (online)
ISBN 978-82-536-1544-8 (pdf)

SINTEF Academic Press
Address: Forskningsveien 3 B
PO Box 124 Blindern
N-0314 OSLO
Tel: +47 73 59 30 00
Fax: +47 22 96 55 08

www.sintef.no/byggforsk
www.sintefbok.no

SINTEF Proceedings
SINTEF Proceedings is a serial publication for peer-reviewed conference proceedings on a variety of scientific topics.
The processes of peer-reviewing of papers published in SINTEF Proceedings are administered by the conference organizers and proceedings editors. Detailed procedures will vary according to custom and practice in each scientific community.

PREFACE

This book contains all manuscripts approved by the reviewers and the organizing committee of the 12th International Conference on Computational Fluid Dynamics in the Oil & Gas, Metallurgical and Process Industries. The conference was hosted by SINTEF in Trondheim in May/June 2017 and is also known as CFD2017 for short. The conference series was initiated by CSIRO and Phil Schwarz in 1997. So far the conference has been alternating between CSIRO in Melbourne and SINTEF in Trondheim. The conferences focuses on the application of CFD in the oil and gas industries, metal production, mineral processing, power generation, chemicals and other process industries. In addition pragmatic modelling concepts and bio-mechanical applications have become an important part of the conference. The papers in this book demonstrate the current progress in applied CFD.

The conference papers undergo a review process involving two experts. Only papers accepted by the reviewers are included in the proceedings. 108 contributions were presented at the conference together with six keynote presentations. A majority of these contributions are presented by their manuscript in this collection (a few were granted to present without an accompanying manuscript).

The organizing committee would like to thank everyone who has helped with review of manuscripts, all those who helped to promote the conference and all authors who have submitted scientific contributions. We are also grateful for the support from the conference sponsors: ANSYS, SFI Metal Production and NanoSim.

Stein Tore Johansen & Jan Erik Olsen

Organizing committee:

Conference chairman: Prof. Stein Tore Johansen
Conference coordinator: Dr. Jan Erik Olsen
Dr. Bernhard Müller
Dr.Sigrid Karstad Dahl
Dr.Shahriar Amini
Dr.Ernst Meese
Dr.Josip Zoric
Dr.Jannike Solsvik
Dr.Peter Witt

Scientific committee:

Stein Tore Johansen, SINTEF/NTNU
Bernhard Müller, NTNU
Phil Schwarz, CSIRO
Akio Tomiyama, Kobe University
Hans Kuipers, Eindhoven University of Technology
Jinghai Li, Chinese Academy of Science
Markus Braun, Ansys
Simon Lo, CD-adapco
Patrick Segers, Universiteit Gent
Jiyuan Tu, RMIT
Jos Derksen, University of Aberdeen
Dmitry Eskin, Schlumberger-Doll Research
Pär Jönsson, KTH
Stefan Pirker, Johannes Kepler University
Josip Zoric, SINTEF

CONTENTS

MODELLING COMBUSTION OF PULVERIZED COAL AND ALTERNATIVE CARBON MATERIALS IN THE BLAST FURNACE RACEWAY

Martin ÖLUND[1*], Lena S. ÖKVIST[1,2], Lars-Erik FROM[1], Dan SANDSTRÖM[1], Johanna ALATALO[3]

[1] Swerea MEFOS, Process Metallurgy Department, Luleå, Sweden

[2] Luleå University of Technology, Division of Minerals and Metallurgical Research, Luleå, Sweden

[3] LKAB, R&D, Luleå, Sweden

* E-mail: martin.olund@swerea.se

ABSTRACT

The impact of injection lance design and injection materials on the combustion conditions inside the raceway of the blast furnace has been investigated. Operational injection tests in LKAB's Experimental blast furnace have been conducted and data describing particle dispersion and temperatures at the tuyere was gathered. A three-dimensional, multiphase numerical model of pulverized material injection (pulverized coal and alternative carbon materials) was developed in order to increase the understanding of raceway conditions in terms of combustion efficiency and reaction rates. In total two different injection lances and two alternative carbon materials in varying blend ratios with pulverized coal were investigated in the numerical study. Simulation results agreed quite well to the experimental data. Furthermore, simulation results agree with published findings regarding the general effect of material properties of pulverized coal on combustion efficiency.

Keywords: Process metallurgy, Blast furnace, Coal injection, Numerical modelling, Combustion, Gasification

NOMENCLATURE

Latin Symbols

A, A_2	Pre-exponential factors for devolatilization and homogeneous reactions, [1/s]
A_c	Pre-exponential factor for heterogeneous reactions, [kg/m^2.s.Pa]
A_p	Particle surface area, [m^2]
A_{EDM}	Empirical constant for Eddy-dissipation model
a, b	Rate exponents
B_{EDM}	Empirical constant for Eddy-dissipation model
C_1	Diffusion rate constant, [kg/m^2.s.Pa.K$^{0.75}$].
$C_{j,n}$	Molar concentration of species j in the reaction n, [kmol/m^3]
d_p	Particle diameter, [m]
E, E_2, E_c	Activation energy, [J/kmol]
f_s	Mass fraction of reacting solid species
$f_{VM,0}$	Initial volatile matter mass fraction
k, k_2	Kinetic rate, [1/s]
m_a	Mass of ash, [kg]
m_p	Particle mass, [kg]
$m_{p,0}$	Initial particle mass, [kg]
m_{VM}	Mass of volatile matter, [kg]
M_i	Molecule weight of species i, [kg/kmol]
p_g	Bulk partial pressure of the reacting gas species, [Pa]
R	Universal gas constant, [J/kmol.K]
R_c	Heterogeneous reaction rate, [kg/s]
R_D	Diffusion rate, [kg/m^2.s.Pa]
R_K	Kinetic rate, [kg/m^2.s.Pa]
$R_{i,n}$	Finite reaction rate of species i and reaction n, [kg/s]
R_{VM}	Devolatilization rate, [kg/s]
T	Temperature, [K]

Greek Symbols

α, α_2	Yield factors

Sub/superscripts

g	Gas
p	Particle
s	Solid
i	Index i
j	Index j
n	Index n

INTRODUCTION

Tuyere injection of auxiliary reducing agents, mainly pulverised coal (PC), has been used in the past few decades to replace some of the coke used in the blast furnace (BF). The main concept of the BF processes is illustrated in Figure 1. Injection of auxiliary reducing agents aims to decrease the use of coke, lowering the total use of carbon and fossil coals in the process. At the same time, this contributes to lower CO_2 emissions and increases the short term heat level control.

When un-burnt PC (char) passes through the raceway boundary entering the packed coke bed, it is consumed together with coke fines in high temperature regions by reduction with CO_2 in reduction gas and FeO in slag. As char is more reactive than coke, accumulation of coke fines may occur (Ishii, 2000) causing permeability problems, channelling and low gas efficiency. Therefore, a high char burnout in the raceway is needed to overcome those issues (Mathieson et al., 2005, Hutny et al., 1991). High injection rates are requested by industry as well as increased flexibility of the process, making the use of alternative carbon material (ACM) injection a relevant topic. The decrease in CO_2 emissions from the BF process would be

significant by both enabling increased injection rates and replacing fossil auxiliary reducing agents.

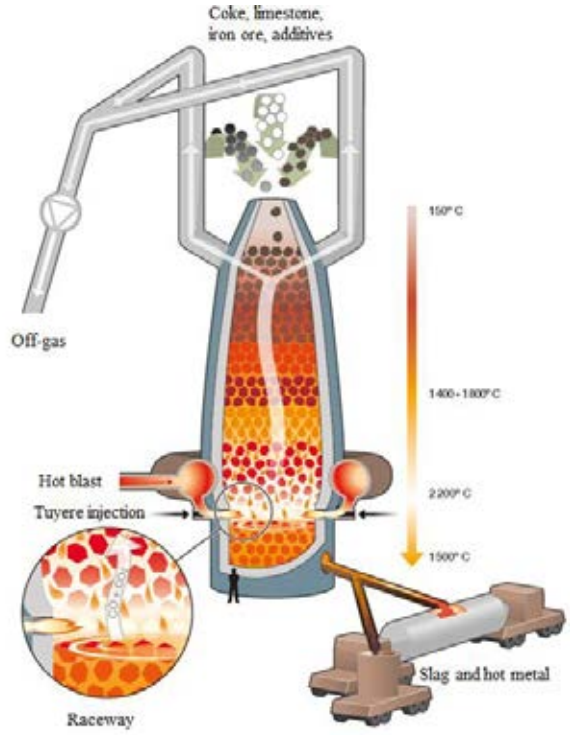

Figure 1: Schematic illustration of the BF process.

The effect of material properties of PC and operational conditions on combustion efficiency has been investigated; combustion efficiency is in general enhanced with increased volatile matter (VM) in PC, decreased particle size, increased blast temperature and enhanced oxygen supply to the PC plume (Pichard, 2001, Ishii, 2000, Mathieson et al., 2005, Shen et al., 2009a). However, PC with lower VM has usually higher replacement ratio to coke (Sundqvist-Ökvist et al., 2016, Ishii, 2000), i.e. more carbon will be converted for the same injection rate even if the combustion efficiency decreases.

The injection system for auxiliary reducing agents varies from BF to BF; hence optimization to enhance the oxygen supply to the PC plume has to be customized (Gudenau et al., 1994). By enhancing particle dispersion the contacting chance for particles and oxygen in the blast will increase. Using a swirl-tip lance instead of an ordinary coaxial air-cooled lance is one method to increase particle dispersion and oxygen utilization. Installation of a swirl-tip lance under oxy-coal conditions made it possible to increase the PC injection rate at LKAB Experimental BF (EBF) (Hallin and Wikström, 2003) and the concept was found to improve combustion conditions in an industrial BF (Wikström et al., 1996). However, using a swirled annular cooling flow doesn't necessarily enhance particle dispersion. In a numerical study the dispersion was found to increase in the tuyere when turning of the swirled cooling flow (Majeski et al., 2012). It must be noted that the thermal effect on the lance by such implementation was not investigated in the study. The purpose of implementing the cooling flow is to prevent excessive heating of the injection lance and thereby prolong lifetime, hence this action might be unrealistic to implement by practical reasons.

Combustion within the tuyere and the raceway cavity is a complex process where multiphase flow in high velocity conditions interacts with intricate chemistry. The requirement of stable operation makes comprehensive research difficult to implement on industrial BFs. Therefore, experiments in laboratory scale (e.g. Vamvuka et al., 1996) and pilot scale are widely used. A compilation of pilot scale test rigs used for evaluation of coal combustion are described by Mathieson et al. (2005). Lack of similarities to the complex industrial process, e.g. the present raceway condition where coke interaction affect the dynamics, might obstruct a direct transfer of findings made at a test rigs handling PC coal combustion only. The LKAB EBF provides a quite rare possibility to overcome those obstacles since pilot scale trials can be conducted in an industrial environment. Since the plant was taken into operation in 1997, a total of 32 campaigns have been conducted. General information about EBF construction and operational conditions has been described elsewhere (Sundqvist-Ökvist et al., 2016, Hallin and Wikström, 2003). The similarities to industrial scale BF conditions retain the harsh environment inside the process and limiting process monitoring opportunities. Hence, insight information to fully explain and understand process improvements caused by different actions is difficult to gather. Therefore, the use of computational fluid dynamics (CFD) in combination with available process data provides a comprehensive tool to increase the understanding of the in-furnace phenomena, provided that the process characteristics are fully captured by the applied mathematical formulation.

In practice, by looking into tuyere and injection lance setup, three-dimensional (3D) models are needed to fully resolve the fluid dynamics in the process. A number of 3D models describing combustion of auxiliary reducing agents in BF like conditions have been carried out by different approaches, such as tuyere combustion models (Du et al., 2007, Majeski et al., 2012), tuyere-raceway combustion models (Guo et al., 2005, Shen et al., 2009, Shen et al, 2016) and tuyere-raceway-coke bed combustion models (Shen et al., 2011, Shen et al., 2012, Maier et al., 2014). Tuyere combustion models have a great potential to resolve the particle dispersion in detail due to the relatively small computational domain. However, the geometrical representation of the raceway region has been stated to have a major impact on the particle dispersion (Mathieson et al., 2005), meaning that results from tuyere combustion models cannot be transferred directly to make conclusions about the overall combustion efficiency in the combustion zone of the BF. In the tuyere-raceway models, the raceway was simplified by a cylindrical combustion chamber where its diameter was enlarged compared to the tuyere diameter. This model approach gives the opportunity to resolve the free shear flow (jet) in the raceway region and capture the effect on particle dispersion and combustion efficiency. Interaction with coke was neglected for those three tuyere-raceway combustion models, chemical reactions and gas composition were direct results of PC combustion and gasification only. The tuyere-raceway-

coke bed combustion models include combustion of coke in the packed coke bed. Raceway shape was not calculated explicitly, but defined as a boundary condition to limit computational efforts. The raceway was represented by a balloon shaped cavity (total void) by Shen et al., (2011, 2012a, 2012b), while Maier et al. (2014) used a more circular shape with gradients in void fraction in the raceway boundary. Even though both definitions were based on literature sources, there was a significant difference in gas flow field in the raceway cavity between both models. Shen found that low speed recirculation of small auxiliary reduction agent particles occurred due to gas recirculation and strongly affected the combustion conditions while Maier et al. (2014) did not stated any gas recirculation. However, the model presented by Maier included coke bed movement and showed that inter-phase momentum transfer made coke particles recirculating in the upper part of the raceway falling into the jet and being partly combusted in the blast. This behaviour has been reported earlier from experimental observations (Kase et al., 1982) and has also been observed within the experiments conducted in connection to this study. Hence, the model presented by Maier et al. (2014) is the only one of the reviewed models that has captured this behaviour.

The CFD model presented in this paper follows the tuyere-raceway modelling approach in order to ensure detailed particle trajectories in the blast. In extension to similar models, coke interaction and subsequent chemical reactions are included to properly evaluate the combustion in BF raceway like conditions.

MODEL DESCRIPTION

Gas-solid flow

The CFD simulations where carried out using the software platform ANSYS FLUENT, release 16.2. The continuous phase was modelled by a set of 3D, steady state Reynolds average Navier-Stokes (RANS) equations with a realizable k-ε turbulence model using enhanced wall treatment. Also the energy equation and the species transport equation were solved in addition to the RANS-equations. The Discrete Ordinates (DO) radiation model was enabled to solve the radiative heat transfer equation. The Euler-Lagrange approach was used to model the dynamics of the multiphase flow, where the solid phase was solved for steady state by tracking a certain number of spherical particles throughout the computational domain. The particles could exchange mass, momentum and energy with the continuous phase. A stochastic tracing model was used to predict the dispersion of the discrete phase due to turbulence. The particle radiation interaction model was enabled to involve the particles in the radiation model. A Rosin-Rammler particle diameter distribution (RRD) was used to simulate the particle size distribution (PSD) data obtained from material screening.

Chemical reactions

The conversion of pulverized auxiliary reduction agents is defined by four steps considering pre-heating, devolatilization, homogenous reactions (gas-gas reactions) and heterogeneous reactions (gas-particle surface reactions). An outline of the considered chemical reactions is presented in Table 1, where (R5) and (R6) is the reversible water-gas shift reaction.

Table 1: Chemical reactions considered.

Devolatilization	
$Raw\ coal \begin{matrix}\rightarrow Volatile\ Matter\ (VM)\\ \rightarrow Char\ (C_{<s>}) + Residue\ (Ash)\end{matrix}$	**(R1)**
Homogenous reactions	
$VM + O_2 \rightarrow Products$	**(R2)**
$CO + 0.5\ O_2 \rightarrow CO_2$	**(R3)**
$H_2 + 0.5\ O_2 \rightarrow H_2O$	**(R4)**
$CO + H_2O \rightarrow CO_2 + H_2$	**(R5)**
$CO_2 + H_2 \rightarrow CO + H_2O$	**(R6)**
Heterogeneous reactions	
$C_{<s>} + 0.75\ O_2 \rightarrow 0.5CO + 0.5CO_2$	**(R7)**
$C_{<s>} + CO_2 \rightarrow 2\ CO$	**(R8)**
$C_{<s>} + H_2O \rightarrow CO + H_2$	**(R9)**

Kinetic parameters for reaction (R1), (R7) and (R8) were deduced from thermogravimetric analysis (TGA), where the sample mass was logged over time in different atmospheres. The same TG program was used for all evaluated materials, i.e. the heating rate was equal. The measured kinetic rate was then adjusted to BF-like conditions by normalizing the pre-exponential factors to a higher ambient temperature. Details of the experimental setup can be found elsewhere (Sundqvist-Ökvist et al., 2016).

Devolatilization

Devolatilization starts when the combusting particle reaches the vaporization temperature and remains while the mass of the particle, m_p, exceeds the mass of non-volatiles in the particles:

$$m_p > \left(1 - f_{VM,0}\right) m_{p,0} \quad \textbf{(1)}$$

where $f_{VM,0}$ is the mass fraction of VM from the proximate analyse and $m_{p,0}$ is the initial particle mass. Depending of the behaviour of the material analysed in the TGA, either a single kinetic rate model or a two-competing rate model has been considered to simulate the devolatilization rate of the evaluated injection agent. The single kinetic rate model (Badzioch and Hawksley, 1970) assumes the devolatilization rate, R_{VM}, has a first-order dependency of remaining mass of VM, m_{VM}, in the particle:

$$R_{VM} = \frac{dm_{VM}}{dt} = k m_{VM} \quad \textbf{(2)}$$

where dm_{VM} is the mass change of VM, dt is change in time and k is the kinetic rate constant, defined by the Arrhenius equation:

$$k = A e^{-\frac{E}{RT}} \quad \textbf{(3)}$$

where A is the pre-exponential factor, E is the activation energy, R is the universal gas constant and T is the temperature. The competing rate model (Kobayashi et al., 1976) assume that two competing kinetic rates, k and k_2, controls the devolatilization rate over different temperatures. The two kinetic rates are weighted to yield an expression for the devolatilization:

$$R_{VM} = (\alpha k + \alpha_2 k_2)(m_p - m_a) \quad \textbf{(4)}$$

where α and α_2 are yield factors and m_a is mass of ash .

Homogenous reactions

The rates of homogeneous reactions are determined by either the kinetics or turbulent mixing. The finite reaction rate model calculates the reaction rate, $R_{i,n}$, for species i and reaction n as:

$$R_{i,n} = M_i k [C_{j,n}]^{a+b} \quad \textbf{(5)}$$

where M_i is the molecule weight of species i, k is the kinetic rate following the Arrhenius approach as described in equation (3), $C_{j,n}$ is the molar concentration of species j in reaction n, a and b are rate exponents. Reaction rate due to turbulent mixing is determined by the Eddy-dissipation model (EDM) (Magnussen and Hjertager, 1976), which requires input of two empirical constants; notated as A_{EDM} and B_{EDM} in this paper. The net reaction rate is taken as the minimum of these two rates. In practice, the finite rate acts as a kinetic switch, preventing reaction before the flame holder. Once the flame is ignited, the Eddy-dissipation rate is generally smaller than the Arrhenius rate, and the reactions are mixing limited.

Heterogeneous reactions

Heterogeneous reactions of PC/ACM and coke with gas species are considering oxidation and gasification with CO_2 and H_2O. Therefore, a multiple surface reactions model was applied. The model assumes that the particle surface reaction rate, R_C, is determined either by the kinetic rate, R_K, or by the diffusion rate, R_D, such as:

$$R_C = A_p f_s p_g \frac{R_K R_D}{R_K + R_D} \quad \textbf{(6)}$$

where A_p is the particle surface area, f_s is the mass fraction of reacting solid species in the particle and p_g is the bulk partial pressure of the reacting gas species. The kinetic rate follows the Arrhenius approach as described in equation (3). The diffusion rate is defined as:

$$R_D = C_1 \frac{T_m^{0.75}}{d_p} \quad \textbf{(7)}$$

where C_1 is the diffusion rate constant, d_p is the particle diameter and T_m is the mean value of particle surface temperature and bulk gas temperature. This model is based on oxidation studies of char particles, but it is also applicable to gas-solid reactions in general, not only to char oxidation reactions.

SIMULATION CONDITIONS

Computational domain

The computational domain, shown in Figure 2, corresponded to the lance and tuyere geometry of the EBF. The main focus when creating the computational domain was to minimize the control volume, without changing the nature of the flow. Initial temperature and velocity of injected material (gas and particles) are important for the combustion conditions. Therefore, the flow in the lance is modelled completely inside the blowpipe-tuyere region, allowing fully developed velocity profiles and temperature increase by convective and radiant heat transfer from the blast respectively the downstream combustion. Mass flow inlets were applied for the blast, cooling gas, carrying gas and auxiliary reducing agents. The raceway cavity was simplified as a cylinder with a length specified in proportion to the furnace diameter. A pressure outlet with a backflow temperature of 1600°C was applied as boundary condition on the outer surface, the upper part also served as a mass flow inlet for discrete particles (coke). A consequence by applying a pressure outlet with constant gauge pressure all over the cylinder surface was that no recirculation of reaction products and/or un-burned particles could occur. However, findings in literature are inconsistent regarding gas and particle (auxiliary reducing agents) recirculation and its effects on combustion conditions in the raceway cavity. Recirculation was either non-existing (Maier et al., 2014), rather small (Zhang et al., 2010) or significant for evaluation of combustion efficiency (Shen et al., 2012). Hence, no definitely recommendations on model setup in this area could be deduced from the reviewed literature.

The computational domain and the boundary conditions applied were assumed to capture enough of the main process conditions without compromising on the details of particle trajectories to be able to evaluate alternative lance designs and injection of ACMs. The computational domain was discretized by an unstructured grid with prism layers in the near-wall region and locally refinements in the lance and close to the lance tip, see Figure 3.

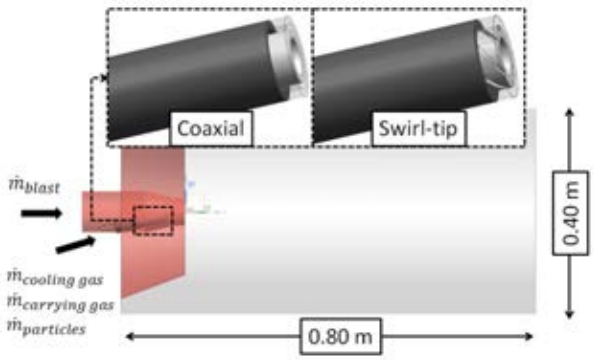

Figure 2: Computational domain and evaluated lance designs seen from the right. The tip (5 mm) of the outer lance pipe is illustrated as transparent to demonstrate the difference in design.

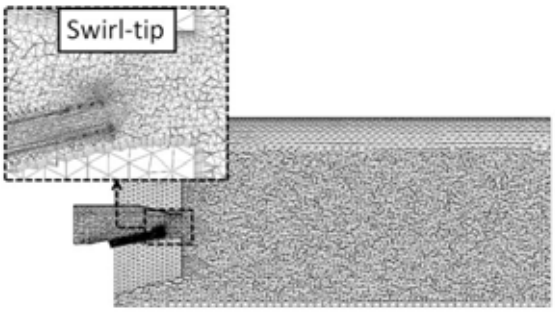

Figure 3: Lance parallel cross-section of the discretized computational domain seen from the right.

Material properties and boundary conditions

In experimental trials (EBF campaign no. 31) three different auxiliary reducing agents were injected: one type of PC, activated lignite coke (ALC) and torrefied biomass (BIO). Material analysis, heating values and vaporization temperature (from TGA) are presented in Table 2. Evaporation of moisture was not considered in the model formulation of chemical reactions, instead the lower heating value was applied to calculate the heat of combustion.

Oxidation of VM, reaction (R2) in Table 1, is dependent of the material properties. Considered oxidation reaction, deduced from the material analysis, for each material is presented in Table 3.

Table 2: Material analysis.

	PC	ALC	BIO
Proximate analysis [wt%]			
VM	18.4	3.1	50.3
Char	69.6	87.0	47.2
Ash	10.8	8.7	0.9
Moisture	1.2	1.15	1.62
Ultimate analysis [wt%]			
S	0.3	0.4	0.0
C	88.6	98.9	71.1
H	4.4	0.2	5.1
O	4.5	0.1	23.7
N	2.2	0.4	0.1
Lower heating value [kJ/kg]	30.5	30.3	27.1
Vaporization temp. [°C]	384	616	276

Table 3: Considered oxidation of VM.

Devolatilization	
$1\,VM_{PC} + 3.37\,O2 \rightarrow 1.62\,CO + 0.47\,CO_2 + 4.74\,H_2O + 0.17\,N2 + 0.02\,SO_2$	**(R2a)**
$1\,VM_{ALC} + 2.58\,O2 \rightarrow 2.29\,CO + 0.66\,CO_2 + 1.31\,H_2O + 0.19\,N2 + 0.17\,SO_2$	**(R2b)**
$1\,VM_{BIO} + 1.71\,O2 \rightarrow 1.58\,CO + 0.46\,CO_2 + 2.23\,H_2O + 0.003\,N2 + 0.00\,SO_2$	**(R2c)**

Table 4: Boundary conditions for the CFD model, based on the operational conditions of the EBF.

Injected auxiliary reducing agent	
Total flow rate [kg/s]	0.021
Temperature [°C]	47
Carrier gas (N_2)	
Flow rate [kg/s]	0.0035
Temperature [°C]	47
Cooling gas (air)	
Flow rate [kg/s]	0.0097
Temperature [°C]	27
O_2 and $H_2O_{(g)}$ mole fractions [-]	0.21/0.0
Blast (oxygen enriched air)	
Flow rate [kg/s]	0.183
Temperature [°C]	1097
O_2 and $H_2O_{(g)}$ mole fractions [-]	0.285/0.019
Top gas pressure [Bar]	2.01

The particle size distribution from material screening is presented in Figure 4 together with the mathematical representation used in the CFD model. The applied boundary conditions are presented in Table 4. During the EBF trials the operational conditions were kept constant, except in terms of lance type and blend ratio of PC/ALC/BIO.

CFD model setup should be close to process conditions to evaluate PC and ACM in terms of combustion efficiency inside the BF raceway. Interaction of coke in the EBF raceway is illustrated in Figure 5, hence coke particles need to be included in the model formulation. However, coke flow rate in the raceway is difficult to measure, instead the assumption that the oxygen content should reach zero when reaching the raceway boundary is used to specify coke boundary conditions. The properties of coke are chosen similar to the coke used in the EBF. The content is considered to be carbon and ash, VM is neglected due to the initial low VM content from the material analysis (<1wt%). Spherical coke particles with a uniform diameter of 15.0 mm and a temperature of 1600°C is injected through the top half of the raceway, in the normal direction, with a flow rate of 1.00 kg/s and an initial velocity of 0.50 m/s. Activation energy for combustion and gasification with CO_2 is taken from related literature (Shen et al., 2010).

Table 5 presents the six different conditions evaluated in the parametric CFD study, where five cases correspond to operational conditions from experimental trials. Case 6 was decided to be evaluated additionally in the CFD model due to its potential to decrease the net CO_2 emissions from the BF process. Considered parameters to describe chemical reactions in the CFD model are presented in Table 6.

Table 5: Boundary conditions for parametric study.

Case	Lance type	Blend PC/ALC/BIO
1. Coaxial PC	Coaxial	100/0/0
2. Swirl PC	Swirl-tip	100/0/0
3. ALC20	Swirl-tip	80/20/0
4. ALC40	Swirl-tip	60/40/0
5. BIO20	Swirl-tip	80/0/20
6. BIO100*	Swirl-tip	0/0/100

* not evaluated in the experimental trials

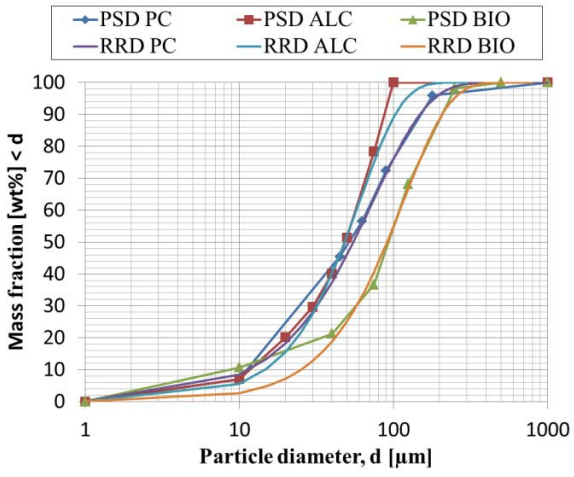

Figure 4: Particle size distribution and mathematical representation by a Rosin-Rammler distribution.

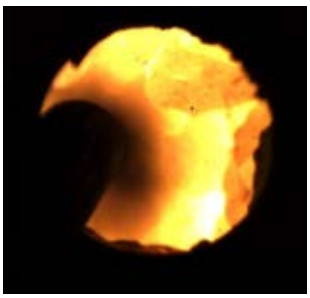

Figure 5: Single frame from high-speed monitoring of tuyere injection in the EBF.

Table 6: Parameters as input in chemical reaction models.

Devolatilization				
	PC	ALC	BIO	
$A_{(R1)}$	1.05E+09	2.30E+13	1.42E+11	
$E_{(R1)}$	9.93E+07	1.85E+08	9.40E+07	
$\alpha_{(R1)}$	0.184	-	-	
$A_{2(R1)}$	1.29E+12	-	-	
$E_{2(R1)}$	1.74E+08	-	-	
$\alpha_{2(R1)}$	1.00	-	-	
Homogenous reactions				
$A_{(R2)}$	2.12E+11			
$E_{(R2)}$	2.03E+08			
$A_{(R3)-(R6)}$	1.00E+15			
$E_{(R3)-(R6)}$	1.00E+08			
A_{EDM}	4.00			
B_{EDM}	0.500			
Heterogeneous reactions				
	PC	ALC	BIO	Coke
$A_{c(R7)}$	2.20	4.40E+05	3.57E+04	2.20
$E_{c(R7)}$	9.79E+07	1.38E+08	1.20E+08	9.00E+07
$A_{c(R8)}$	1.33	22.9	1.88E+6	1.33
$E_{c(R8)}$	1.86E+08	1.69E+08	2.46E+08	2.40E+08
$A_{c(R9)}$	1.5	1.5	1.5	-
$E_{c(R9)}$	1.50E+08	1.50E+08	1.50E+08	-
C_1	5.00E-12	5.00E-12	5.00E-12	2.50E-08

RESULTS

Validation

High-speed video recordings and temperature measurements from EBF campaign no. 31 have been used to validate model results. A visual validation was carried out by comparing high-speed videos with post-processed model images. A contour plot of the particle mass concentration at tuyere outlet is compared to a single frame from the high-speed videos in Figure 6 (presented cases are Coaxial PC and Swirl PC). As can be seen, there is some difference in lance location between the process images and the model images. However, the trends in dispersion are similar for the high-speed images and the model image since the main coal plume area is located perpendicular to the lance outlet for Coaxial PC, while the swirling flow from the swirl-tip makes the main coal plume area located to the right of the lance.

Even though the way of particles dispersion is stated to differ between coaxial and the swirl-tip lance, the image analysis of the high-speed images did not detect any major differences in terms of area of particle dispersion. The area seems to be at equal size by just visually comparing the model images in Figure 6. A more accurate picture is given when removing the injection lances in Figure 7. The difference in particle dispersion becomes hereby obvious.

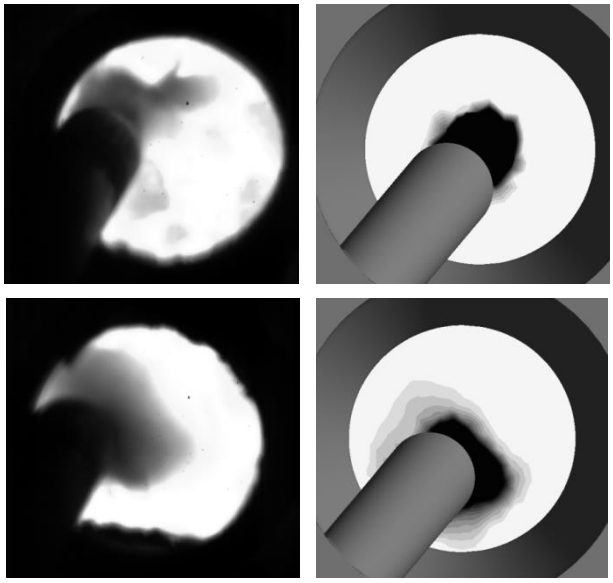

Figure 6: Visual comparison between high-speed image of the EBF process (left) and the CFD model (right), for Coaxial PC (upper) and Swirl PC (lower).

In Figure 8 the average gas temperature for the cross-sectional plane generating the highest value (varies depending on start of combustion, particle dispersion etc.) are compared to spectrometer measurements and theoretical calculations of the raceway adiabatic flame temperature (RAFT). Optical fibres where used to guide light from the tuyere to the spectrometer for the spectrometer measurement.

As expected, RAFT generates the highest temperatures overall. Spectrometer measurements retain the same trend as RAFT, even though the temperature is decreased. The same trend is obtained when comparing CFD model results to RAFT and spectrometer measurements, Coaxial PC has the lowest flame temperature and ALC40 has the highest. The maximum divergence in temperature between spectrometer and CFD model are found for ALC40 where the divergence amounts to 0.9%. Overall, the changes in injected material generate reasonable results. The temperature increase for ALC40 in the model cannot be seen in the same extent as for RAFT and spectrometer measurements. Further, the model seems to underestimate the temperature for Coaxial PC to a minor extent. A possible explanation might be that the coke particles in the raceway region affect the dispersion of PC particles by collisions; increasing the PC dispersion. This effect should be greater for Coaxial PC compared to the Swirl PC due to a less dispersed plume when reaching the raceway region. The effect of particle collision is not included in the model formulation.

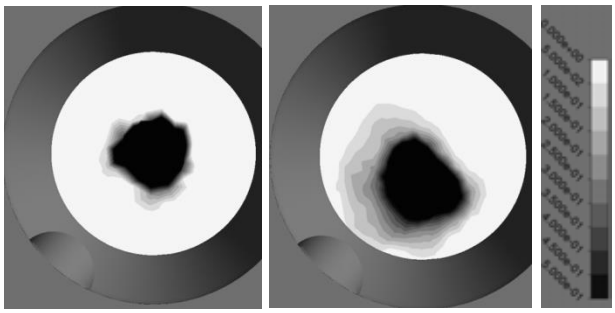

Figure 7: Contour plot of particle mass concentration (kg/m^3) at tuyere outlet, no lance displayed (Coaxial PC left, Swirl PC right)

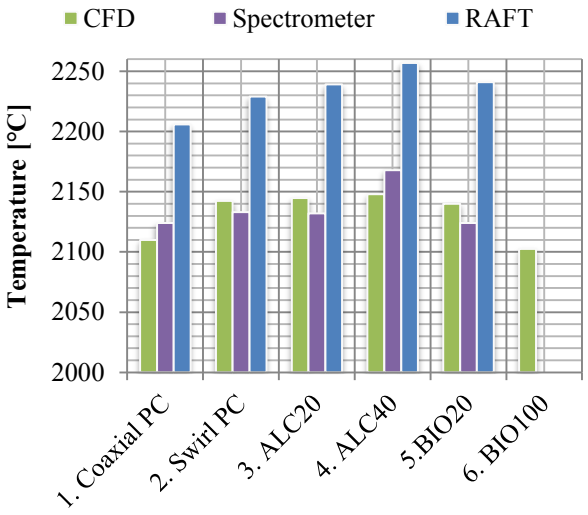

Figure 8: CFD model temperatures compared to spectrometer measurements and RAFT.

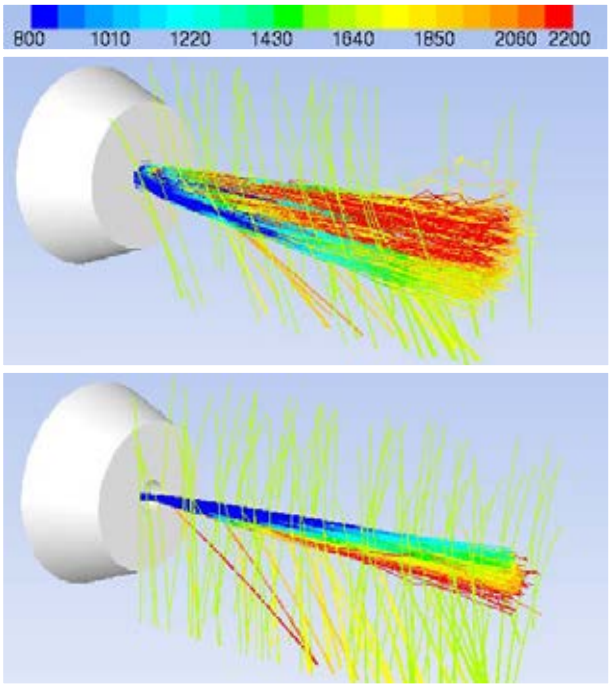

Figure 9: Particle trajectories for Swirl PC (upper) and Coaxial PC (lower) coloured by particle temperature (°C). PC particles enter the raceway through the injection lance inside the tuyere, while coke particles are injected from the top of raceway.

Alternative lance design

Particle trajectories, coloured by particle temperature, of PC and coke for Coaxial PC and Swirl PC are presented in Figure 9. Unlike the image analysis of particle dispersion, the difference in dispersion is clear. The swirl-tip lance increases particle dispersion significantly resulting in earlier ignition (Figure 11**)** and increased carbon conversion of PC (Table 7). Especially carbon converted via combustion is increased by Swirl PC, illustrated in Figure 10. For Swirl PC the heterogeneous reaction rate of combustion is the fastest, followed by carbon solution loss and last gasification with water vapour, while for Coaxial PC the behaviour is vice versa. This might be explained by the differences in particle dispersion, where worse PC dispersion makes larger regions of the blast stream unoccupied and limits the conversion by oxidation. With the current model formulation this oxygen will react with coke, making the total carbon conversion the highest for Coaxial PC (Table 7). This explains why the highest average temperature does not diverge that much. By looking into the reaction rates and comparing the net enthalpy change the difference should be larger if only comparing PC conversion. However, total carbon conversion is not a proper measurement to evaluate the combustion efficiency. One main purpose of injecting auxiliary reducing agents in the raceway is to decrease the total use of carbon, by replacing some of the coke. This should be done by converting as much carbon as possible of the injected material in the raceway region to avoid unstable BF operation.

Alternative carbon materials

For case 2-6 the swirl lance has been used. Differences in combustion efficiency and characteristics are all connected to differences in the properties of the injected materials; such as PSD, analysis and reaction parameters. BIO100 has the earliest start of combustion followed by BIO20, see Figure 11 and Table 7. Start of combustion depends on injected material and lance type used. For the swirl-tip lance, the deciding factor seems to be the VM content in the injected material/blend. As a consequence, the highest carbon burnout of the injected material is reached for the BIO-cases. In general, increased VM leads to increased combustion efficiency in terms of carbon burnout. BIO has larger particle size compared to ALC and PC, which might counter the efficiency enhancement from the increase in VM. The extent of this factor has not been investigated in this work. Further, ALC40 converts the most carbon from the injected materials. The observed behaviour corresponds to earlier findings presented in reviewed literature. However, BIO20 has a higher amount of VM compared to Swirl PC but increases not only the combustion efficiency, but also the carbon conversion. This might be motivated by the synergetic effect; where BIO releases more VM, helping form a higher gas temperature field in an earlier stage promoting PC devolatilization and combustion. This theory is supported by Shen et al. (2009b).

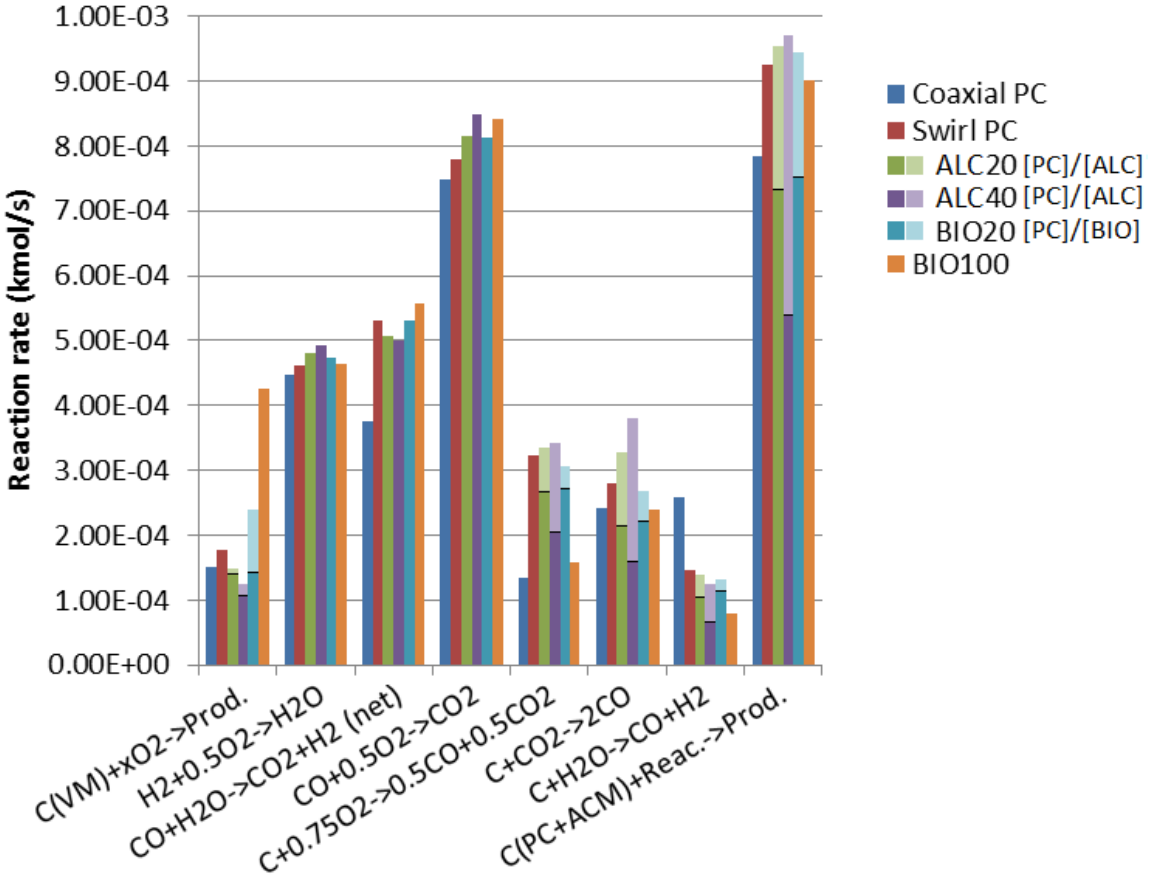

Figure 10: Reaction rates in kmol/s. Cases with blends (ALC20, ALC40 and BIO20) are presented in total rate, where darker shade corresponds to carbon originates from PC and lighter shade to carbon originates from ACM.

Table 7: Combustion characteristics for all evaluated cases.

	Coaxial PC	**Swirl PC**	**ALC20**		**ALC40**		**BIO20**		**BIO100**
PC and ACMs only									
Auxiliary reducing agent	PC	PC	ALC	PC	ALC	PC	BIO	PC	BIO
C in VM converted [g/s]	1.81	2.13	0.10	1.72	0.21	1.29	1.15	1.73	5.15
VM burnout [%]	84.4	99.4	100.0	99.7	100.0	99.8	100.0	99.9	89.6
$C_{<s>}$ converted [g/s]	7.61	9.00	2.57	7.09	4.99	5.22	1.14	7.34	5.73
$C_{<s>}$ burnout [%]	53.3	63.1	69.7	61.9	68.5	60.9	63.5	64.1	64.3
C converted [g/s]	**9.42**	**11.13**	**11.48**		**11.71**		**11.36**		**10.88**
C burnout [burnout]	**57.4**	**67.8**	**67.7**		**67.5**		**70.4**		**74.2**
Including coke									
$C_{<s>}$ in coke converted [g/s]	15.82	11.63	11.98		12.36		11.41		11.84
Total C converted [g/s]	**25.24**	**22.76**	**23.46**		**24.07**		**22.77**		**22.72**
Total C burnout [%]	**3.13**	**2.82**	**2.90**		**2.98**		**2.82**		**2.82**
Other comb. characteristics									
Start of combustion [mm]	146	29	32		35		22		12
Plane position for highest avg. temp. [mm]	490	340	340		390		340		390
Highest avg. temp., $T_{avg.}$ [°C]	**2110**	**2142**	**2145**		**2148**		**2140**		**2102**

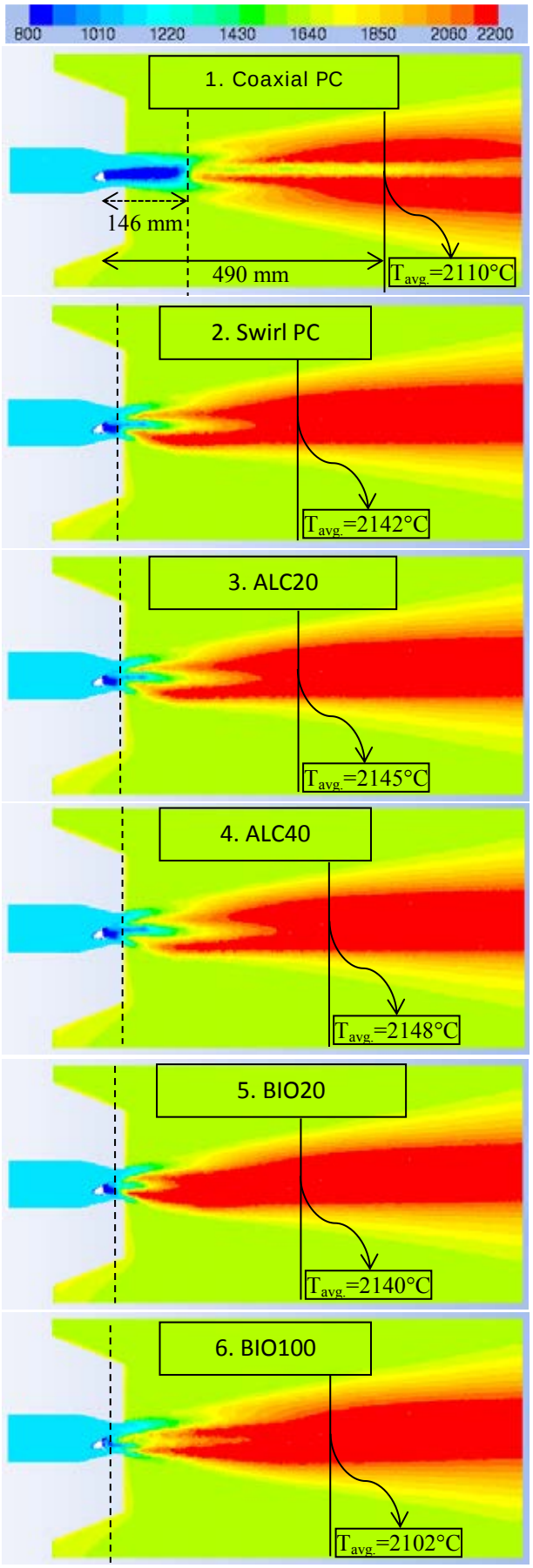

Figure 11: Contour plot of temperature (°C) at cross-sectional plane (tuyere seen from the right). Solid line indicates position of plane for highest average temperature and dashed line indicates start of combustion.

By comparing the flame distribution for the swirl-tip cases in Figure 11 there are some minor differences, most likely explained by differences in PSD between the materials. BIO is deviant in PSD compared to PC and ALC, which might explain the decreased flame distribution close to the tuyere outlet. It will take longer time for the particles to change direction due to the increased momentum. Making the PSD for BIO closer to the other two materials will most likely enhance the combustion efficiency even further**.**

In Table 7 and Figure 11 it can be seen that the highest average temperature is found in different positions downstream the lance tip. Highest average temperatures are found further downstream for Coaxial PC, ALC40 and BIO100 compared to Swirl PC, ALC20 and BIO20 that all have the highest temperature at approximately 340 mm downstream the lance tip. For Coaxial PC, later ignition leads to postponed combustion of solid carbon in PC. The ignition for ALC40 is postponed as well, but to a minor extent. The increased activation energy needed to combust solid carbon in ALC compared to PC is assumed to be the explanation. The same explanation partly applies to BIO100, together with the increased PSD.

The highest average temperature is found for ALC40, while BIO100 generates the lowest. By only comparing the heating value for full combustion the temperature difference appears to be too small. However, the complexity of the process is high and full combustion is not the case. By looking into the reaction behaviour and comparing reaction rates and net enthalpy change this is reasonable.

CONCLUSION

A three-dimensional, steady-state CFD model has been developed to investigate the impact of injection lance design and injection materials on the combustion conditions inside the raceway of the blast furnace. In total, two injection lances and three injection materials where evaluated under uniform operation conditions. A detailed geometric representation of the injection lance and tuyere was included in the model. The model was found suitable for evaluating alternative lance designs and alternative carbon materials for injection in the BF by validation against measurements from experimental trials. The developed modelling technique can advantageously be transferred to any industrial BF.

Compared to the ordinary coaxial lance, the swirl-tip lance was found to significantly enhance the combustion efficiency of PC, increasing carbon conversion and raceway temperature. Model results indicate that the swirl-tip lance enables increased injection rates of auxiliary reducing agents without making any major impact on the tuyere installation. BIO (torrefied biomass) showed overall good results in the CFD model, making it a suitable candidate to reduce the total amount of fossil coal used in the BF process. With a blend of 20 wt% BIO in PC the temperature remained stable and both carbon conversion and combustion efficiency were increased. Further, the low sulphur content in BIO compared to PC reduces the production of sulphur dioxide in the process.

The CFD model presented is a useful tool for BF tuyere injection evaluation by complementing available measurements and providing further insights in the harsh BF process.

ACKNOWLEDGMENTS

The research presented in this paper has been carried out within the project IMPCO RFSR-CT-2012-00002, co-founded by the Research fund for coal and steel, RFCS. The Swedish Energy Agency is greatly acknowledged for additional financial contribution to the project. The paper is a contribution from CAMM, Centre of Advanced Mining and Metallurgy, at Luleå University of Technology supporting the presented research scientifically and economically.

REFERENCES

BADZIOCH, S. and HAWKSLEY, P. G.W., (1970) "Kinetics of thermal decomposition of pulverized coal particles", *Ind. eng. chem. process design and development*, **9**, 521–530.

DU, S-W., CHEN, W-H. and LUCAS, J., (2007) "Performances of pulverized coal injection in blowpipe and tuyere at various operational conditions", *Energy conversion and management,* **48**, 2069-2076.

GUDENAU, H.W., PETERS, M., JOKSCH, M., (1994) "Steigerung de Kohleeinblasrate am Hochofen durch Optimierung der Einblaslanzen", *Stahl und Eisen,* **114**, 69-73.

GUO, B., ZULLI, P., ROGERS, H., MATHIESON, J.G., and YU, A., (2005) "Three-dimensional simulation of flow and combustion for pulverized coal injection", *ISIJ Int.,* **45**, 1272-1281.

HALLIN, M. and WIKSTRÖM. J-O., (2003) "Ways to improve the blast furnace operation – The Use of an Experimental Blast Furnace", *Sci. and tech. of innovative ironmaking for aiming at energy half consumption,* Tokyo, Japan, November 27-28.

HUTNY, W.P., LEE, G.K. and PRICE, J.T., (1991) "Fundamentals of coal combustion during injection into blast furnace", *Prog. Energy Comb. Sci.,* **17**, 373-395.

ISHII, K., (2000) "Advanced pulverized coal injection technology and blast furnace operation", *research group of pulverized coal combustion in blast furnace ironmaking in JSPS 54th Committee.*

KASE, M., SUGATA, M., YAMAGUCHI, K. and NAKAGOME, M., (1982) "Analysis of coke behavior in raceway using endoscope and high-speed camera", *Transactions of the iron and steel inst. of Japan,* **22**, 811-819.

KOBAYASHI, H., HOWARD, J. B. and SAROFIM, A. F., (1976) "Coal devolatilization at high temperatures", *In 16th symp. (Int'l.) on combustion. The combustion institute.*

MAGNUSSEN, B.F. and HJERTAGER, B. H., (1976) "On mathematical models of turbulent combustion with special emphasis on soot formation and combustion", *In 16th symp. (Int'l.) on combustion. The combustion institute*.

MAIER, C., JORDAN, C., FEILMAYR, C., and HARASEK, M., (2014) "Multi-scale modelling of hydrocarbon injection into the blast furnace raceway", *10th int. conf. on CFD in oil & gas, metallurgical and process industries,* SINTEF, Trondheim, Norway, June 17-19.

MAJESKI, A., RUNSTEDTLER, A., D'ALESSIO, J., MACFADYEN, N. and FERRON, K., (2012) "The effects of lance positioning and design on the co-injection of pulverized coal and natural gas into blast furnace", *Ninth int. conf. on CFD in Minerals and process ind.,* CSIRO, Melbourne, Australia, December 10-12.

MATHIESON, J.G., TRUELOVE, J.S. and ROGERS, H., (2005) "Towards an understanding of coal combustion in blast furnace tuyere injection", *Fuel*, **84**, 1229-1237.

Picard, M., (2001) "Pulverized coal combustion in the blast furnace raceway, using a 3D numerical simulation", *Ironmaking Conf. Proc.*, Baltimore.

SHEN, Y., GUO, B. and ZULLI, P., (2009a) "Model study of the effects of coal properties on pulverized coal combustion", *ISIJ int.,* **49**, 819-826.

SHEN, Y.S., GUO, B.Y., YU, A.B., and ZULLI, P., (2009b) "A three-dimensional numerical study of the combustion of coal blends in blast furnace", *Fuel,* **88**, 255-263.

SHEN, Y.S., GUO, B.Y., YU, A.B., AUSTIN, P.R. and ZULLI, P., (2011) "Three-dimensional modelling of in-furnace coal/coke combustion in a blast furnace", *Fuel,* **90**, 728-738.

SHEN, Y.S., YU, A.B., AUSTIN, P.R. and ZULLI, P., (2012a) "CFD study of in-furnace phenomena of pulverized coal injection in blast furnace: Effects of operating conditions", *Powder technology,* **223**, 27-38.

SHEN, Y., YU, A., AUSTIN, P. and ZULLI, P., (2012b) "Modelling in-furnace phenomena of pulverized coal injection in ironmaking blast furnace: Effects of bed porosities", *Minerals engineering,* **33**, 54-65.

SHEN, Y.S. and YU, A.B., (2016) "Modelling of injecting a ternary coal blend into a model ironmaking blast furnace", *Minerals engineering,* **90**, 98-95.

SUNDQVIST-ÖKVIST, L., ÖLUND, M., SANDSTRÖM, D., FROM, L-E. and ALATALO, J., (2016) "Impact on combustion conditions from tuyere injection settings", *7th European coke and ironmaking congress,* Linz.

VAMVUKA, D., SCHWANEKAMP, G. and GUDENAU, H.W., (1996) "Combustion of pulverized coal with additives under conditions simulating blast furnace injection", *Fuel,* **75**, 1145-1150.

WIKSTRÖM, J-O., SKÖLD, B-E. and KÄRSRUD, K., (1996) "SSAB/MEFOS oxy-coal system - 3 years of industrial experience", *55th Ironmaking Conf. Proc*., Pittsburgh, USA.

ZHANG, S., BAI, C., WEN, L., QIU, G. and LÜ, X., (2010) " Gas-particle flow and combustion characteristics of pulverized coal injection in blast furnace raceway", *Journal of iron and steel research, int.,* **17**, 8-12.